Astronomy & Astrophysics manuscript no. paper˙v2
April 21, 2008

LETTER TO THE EDITOR

The first VLBI image of an Infrared-Faint Radio Source

E. Middelberg[1], R. P. Norris[2], S. Tingay[3], and C. Phillips[2]

[1] Astronomisches Institut, Ruhr-Universität Bochum, Universitätsstr. 150, 44801 Bochum, Germany
e-mail: middelberg@astro.rub.de
[2] Australia Telescope National Facility, PO Box 76, Epping NSW 1710, Australia
e-mail: ray.norris@csiro.au, chris.phillips@csiro.au
[3] Department of Imaging and Applied Physics, Curtin University of Technology, Bentley, Western Australia, Australia
e-mail: s.tingay@ivec.org

Received, accepted

ABSTRACT

Context. To investigate the joint evolution of active galactic nuclei and star formation in the Universe.
Aims. In the 1.4 GHz survey with the Australia Telescope Compact Array of the Chandra Deep Field South and the European Large Area ISO Survey - S1 we have identified a class of objects which are strong in the radio but do have no detectable infrared and optical counterparts. This class has been called Infrared-Faint Radio Sources, or IFRS. 51 sources out of 2002 detected have been classified as IFRS. It is not known what these objects are.
Methods. To address the many possible explanations as to what the nature of these objects is we have observed four sources with the Australian Long Baseline Array.
Results. We have detected and imaged one of the four sources observed. Assuming that the source is at a high redshift, we find its properties and morphology in agreement with properties of Compact Steep Spectrum sources. However, due to the lack of optical and infrared data the constraints are not particularly strong.

Key words. Galaxies:active, Galaxies: peculiar

1. Introduction

Infrared-Faint Radio Sources (IFRS) were recently discovered as a class by Norris et al. (2006), and may be related to the Optically Invisible Radio Sources (OIRS) identified by Higdon et al. (2005). IFRS are radio sources which have no counterparts in infrared images from the *Spitzer* Wide-Area Extragalactic Survey (SWIRE) between 3.6 μm and 24 μm, and are discovered in arcsec-scale radio observations. They are unexpected because it was thought that any galaxy which is detected in radio observations should be detected in the infrared with relatively short integrations. Norris et al. (2006) and Middelberg et al. (2008) together identified 53 such sources out of 2002 (2.7 %) detected in the ATLAS survey, co-located with the SWIRE survey. Most of these sources have flux densities of only a few hundred microjansky, but some are strong and have flux densities of more than 20 mJy. Stacking 3.6 μm *Spitzer* images at the positions of 22 IFRS, Norris et al. (2006) were unable to make a detection in the averaged image and so demonstrated that IFRS are well below the detection threshold of the SWIRE survey.

The nature of IFRS and the reason for their faintness at infrared wavelengths is unclear. Possible explanations are that (i) these sources are extremely redshifted Active Galactic Nuclei (AGN); (ii) they are dust-rich, extremely obscured galaxies which makes them invisible in the infrared; (iii) they are lobes of nearby, unidentified radio galaxies; or (iv) they are an unknown type of galactic or extragalactic object. Because IFRS have so far only been detected at radio wavelengths it is not possible to measure their redshifts, as spectroscopy requires sub-arcsecond positional accuracy, which the radio observations cannot provide. Also, the comparatively low resolution of the radio images makes it impossible to select the correct optical counterpart, because the corresponding optical observations are deep, and hence confusion-limited.

A promising route to find out more about IFRS are radio observations with Very Long Baseline Interferometry (VLBI). VLBI observations are sensitive only to very compact structures with brightness temperatures of the order of 10^6 K or more, which are unambiguous signposts of AGN activity. They also yield, when astrometric calibrators are used, positions accurate to milliarcseconds, and milli-arcsecond-scale morphologies which can be interpreted in terms of the emission mechanism at work.

Here we present VLBI observations of four IFRS discovered in the ATLAS/ELAIS field (Middelberg et al. 2008). We selected S427 and S509 because they were the strongest IFRS in the ATLAS/ELAIS field, and S775 because it is very extended on arcsecond scales, showing structures reminiscent of lobes and jets frequently seen in AGN. After the observations it was discovered that the weak IFRS S433 was located only 24.6 arcsec north-east of S427 (Fig. 1), and was well within the field of view of the VLBI array. The details of the sources observed are listed in Table 1.

2. Observations

We observed the IFRS with the Australian Long Baseline Array (LBA) in phase-referencing mode. On 24 March 2007 the participating antennas were the Australia Telescope Compact Array (ATCA), the 64 m Parkes telescope, the 22 m Mopra telescope and the 26 m telescope near Hobart. On 21 June 2007 the same array was used, plus the 30 m telescope at Ceduna. The ATCA,

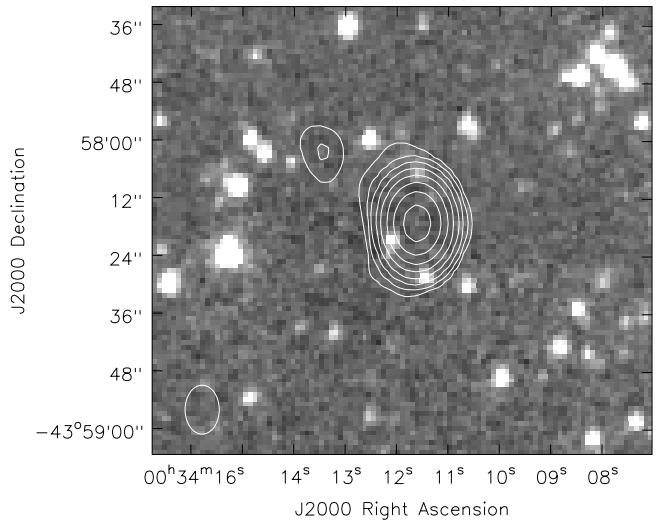

Fig. 1. Contour plot of the ATLAS/ELAIS image of S427 superimposed on the 3.6μm *Spitzer* image made as part of the SWIRE survey (Lonsdale et al. 2003). Contours are drawn at 0.1 mJy×(1, 2, 4, ...) and the restoring beam was 10.3×7.2 arcsec. The nearest infrared source, located towards the south-east, is more than 6 arcsec away, making it very unlikely to be the infrared counterpart. Source S433, visible as a two-contour object 24.6 arcsec north-east of S427, also was classified as an IFRS. It has a flux density of 245 μJy.

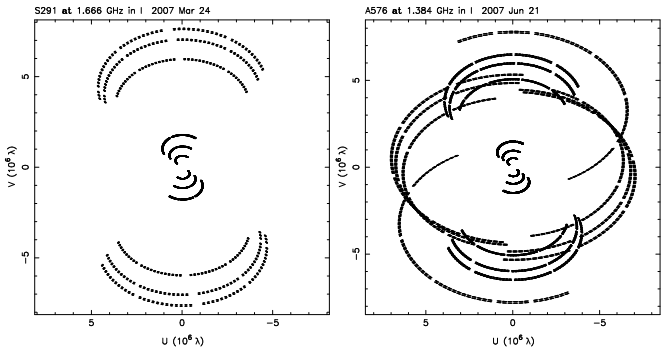

Fig. 2. Plots showing the (u, v) coverage of the observations of S427 on 24 March (left) and of S775 on 21 June (right).

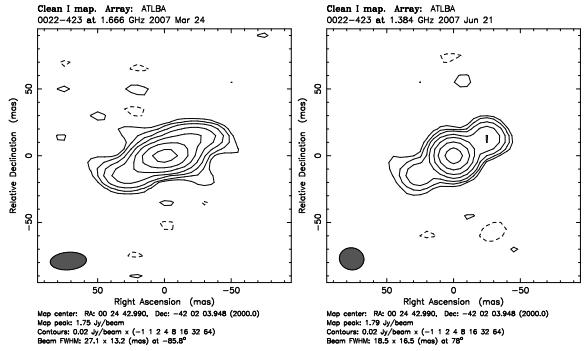

Fig. 3. Contour plots of the phase calibrator 0022-423 observed on 24 March (left) and 21 June (right). Contours are drawn at 20 mJy×(-1, 1, 2, 4, ...) and the restoring beam was 27.1 mas×13.2 mas (left) and 18.5 mas×16.5 mas (right). The observations on 21 June used a slightly improved position for the calibrator.

Parkes and Mopra telescopes recorded a total bandwidth of 64 MHz using 2-bit sampling, subdivided in 16 MHz wide IF channels. Both right-hand and left-hand circular polarization were recorded. The Hobart and Ceduna telescopes recorded a total bandwidth of 32 MHz with the same setup. Both observing runs lasted for 12 h. The total (u, v) coverage of the two observing runs is shown in Fig. 2.

On 24 March, the coordinates of IFRS S427 and S509 were observed for 5 min each, followed by a 3 min-scan on the nearby phase calibrator 0022-423, which has an arcsec-scale flux density (monitored with the ATCA) of 2.82 Jy. S433 was also in the field of view of these observations. On 21 June, 8 min-scans of the IFRS S775 were followed by a 3 min-scan of the same calibrator. One of the fringe finders 1921-293 and 0104-408 was observed every two hours in either run. The predicted baseline sensitivity for a 3 min calibrator scan was 3 mJy on the least sensitive baseline between Mopra and Hobart. The LBA sensitivity calculator[1] predicts image sensitivities of around 50 μJy for the targets.

3. Calibration

The lower and upper 10 out of 64 channels in each IF had low amplitudes and were flagged. Also, after source changes the correlator produced data although the antennas had not yet arrived at the source positions, requiring the flagging of 30 s of the beginning of all scans, and occasionally more. A short section of a fringe-finder observation was fringe-fitted to obtain residual and instrumental delays, and phase offsets for each IF and polarization separately. These solutions were applied to the entire data set, and allowed averaging across the band in the subsequent fringe-fitting of the phase calibrator. The phase calibrator was detected on all baselines throughout the experiments with high SNR. Initial amplitude calibration was carried out using $T_{\rm sys}$ values measured during the observations, and known antenna gains. The phase calibrator was then imaged in Difmap (Shepherd 1997). Amplitude self-calibration was performed in Difmap with a 720 min solution interval, yielding small (<20 %) corrections for the antenna gains. The complex gains from this procedure were then applied to the targets. Contour plots of the calibrator are shown in Fig. 3. An area of 2″ centred on the targets' arcsec-scale emission was imaged to look for the sources.

[1] http://www.atnf.csiro.au/vlbi/calculator

4. Results and discussion

Only one of the three targets, S427, was detected with good SNR. The other three fields were completely devoid of emission. In the case of S433 the loss of sensitivity due to wide-field effects (bandwidth smearing, time smearing, and primary beam attenuation) is of the order of only a few percent on the longest baselines, and hence is negligible. Therefore its non-detection is just as significant as the other non-detections.

4.1. S427

The image of S427 in Fig. 4 displays a slightly extended point source, with the highest sidelobes at a level of 0.3 mJy. The peak flux density in the image is 8.2 mJy and the integrated flux density is 12.5 mJy. The limited (u, v) coverage defied attempts to develop a more detailed model, and caused the noise in regions away from the source to be dominated by sidelobes rather than

Table 1. Source parameters and results from our observations. Column 1: source name; column 2: formal IAU designation, which for brevity we do not use elsewhere in this paper; columns 3-4: coordinates used in the observations. The target coordinates differ from those published in Middelberg et al. (2008) because they were taken from an earlier version of the image; column 5: ATCA 1.4 GHz flux density by Middelberg et al. (2008) in mJy; column 6: integrated flux density found in the VLBI images in mJy; column 7: peak flux density of the VLBI images in mJy; column 8: rms noise in the VLBI images in mJy. The peaks in the last three sources all are below $5\,\sigma$, and the locations of the brightest pixel does not coincide with the arcsec-scale source position.

Source	IAU designation	RA	Dec	$S_{1.4\,\mathrm{GHz}}$ mJy	S_{VLBI} mJy	$S_{\mathrm{VLBI,max}}$ mJy	rms mJy
(1)	(2)	(3)	(4)	(5)	(6)	(7)	(8)
0022-423	PKS 0022-423	00:24:42.989741	-42:02:03.94796	2820			
S427	ATELAIS J003411.59-435817.0	00:34:11.59	-43:58:17.036	21.4	12.5	8.2	0.14
S509	ATELAIS J003138.63-435220.8	00:31:38.64	-43:52:20.824	22.2	...	0.27	0.065
S433	ATELAIS J003413.43-435802.4	00:34:13.43	-43:58:02.470	0.2	...	0.27	0.069
S775	ATELAIS J003216.05-433329.6	00:32:16.01	-43:33:37.092	3.6	...	0.26	0.055

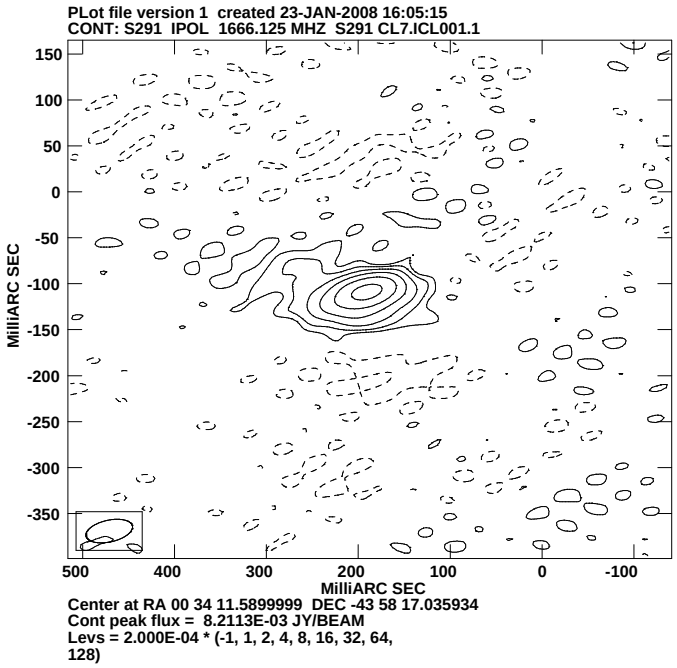

Fig. 4. Contour plot of the IFRS S427. Contours are drawn at 0.2 mJy×(-1, 1, 2, 4, ...) and the restoring beam was 51.7 mas×23.6 mas.

receiver noise. On the longest baselines the source has a flux density of 7 mJy, from which we infer a minimum brightness temperature of $T_{\mathrm{B,min}} = 3.6 \times 10^6$ K, indicating non-thermal emission. We therefore conclude that the source contains an AGN.

S427 has an arcsec-scale flux density of 21.4 mJy (Middelberg et al. 2008), 58 % of which we recovered on baselines longer than 500 kλ, or on scales smaller than 410 mas, and 33 % of which are detected on baselines longer than 6.5 Mλ, or on scales smaller than 32 mas. Following the discussion by Norris et al. (2007), we model the emission of S427 assuming it has redshifts of $z = 1$ and $z = 7$ (the results of which we give in brackets).

The measured flux densities need to be corrected for redshift (k-correction) and spectral index (α, $S \propto \nu^{\alpha}$). From a 2.3 GHz follow-up survey of the ATLAS/ELAIS field currently being conducted by us with the ATCA, and from the SUMSS survey (Bock et al. 1999) we have obtained two more spectral points for S427. The catalogued flux density from the SUMSS survey at a frequency of 843 MHz and with a resolution of $45'' \times 64''$ was 42.7 mJy, and from our preliminary 2.3 GHz image at a centre frequency of 2.424 GHz and with resolution of $52'' \times 28''$ we have obtained a flux density of 12.5 mJy. We have convolved the 1.4 GHz ATLAS/ELAIS image (with a centre frequency 1.382 GHz and a resolution of $10.3'' \times 7.2''$) with an appropriate Gaussian kernel to generate an image with a resolution matching that at 2.3 GHz, and found a flux density of 22.7 mJy. This is within the errors of the flux density measured from the higher-resolution image and indicates that there is no faint emission on scales of tens of arcsec, as would be expected from a very compact source. The spectral indices therefore can be computed from the full-resolution 1.4 GHz image, and are $\alpha^{843}_{1.382} = -1.39$ and $\alpha^{1.382}_{2.424} = -0.96$.

In the case of S427, a 1.4 GHz flux density of 21.4 mJy corresponds to an observed 5 GHz flux density of 6.3 mJy, which, when corrected for redshift and spectral index, corresponds to a rest-frame 5 GHz luminosity of 6.4×10^{25} W Hz^{-1} (2.7×10^{28} W Hz^{-1} if z=7, using H_0=71, $\Omega_{\mathrm{M}} = 0.27$ and $\Omega_{\mathrm{vac}} = 0.73$). At z=7 this is approximately the luminosty of 3C 273, hence is high (e.g., O'Dowd et al. 2002), but not impossible.

The size of the source can be estimated as follows. In the ATCA image the source was well represented with a Gaussian of $10.62'' \times 7.89''$ in PA 174°. After deconvolution from the restoring beam, the intrinsic source size was found to be $3.30'' \times 2.74''$ in PA 95°. At z=1 the linear scale is 8.0 kpc arcsec^{-1} (5.3 kpc arcsec^{-1}), and so the intrinsic source size is of the order of 24 kpc (16 kpc).

We point out that the position angles of deconvolved sources in the source catalogue by Middelberg et al. (2008) are very evenly distributed and do not appear to be biased in any direction. Hence the orientation of S427, when deconvolved from the restoring beam in the arcsec-scale image, is in agreement with the extension seen in the VLBI image.

It is surprising that S509 has spectral properties which are very similar to S427, with $S_{2.424} = 12.6$ mJy, $S_{843} = 37.6$ mJy, and thus $\alpha^{843}_{1.382} = -1.06$ and $\alpha^{1.382}_{2.424} = -1.01$. Its intrinsic size at 1.4 GHz after deconvolution is $3.48'' \times 2.77''$ in PA 59°. Yet it remains undetected in our VLBI observations which indicates that if it contains an AGN it is comparatively weak or currently inactive.

4.1.1. Is S427 a compact steep-spectrum source?

The size of S427 is comparable to typical sizes of Compact Steep-Spectrum sources (CSS), but larger than typical Gigaherz-Peaked Spectrum sources (GPS) (e.g., O'Dea & Baum 1997).

CSS and GPS sources are very small yet strong radio sources. They are contained within their host galaxies, with CSS source being larger (up to 20 kpc), whereas GPS sources are

smaller than 1 kpc, so that they are smaller than the narrow-line region. The two competing models to explain their properties are that they are either "frustrated" radio galaxies which are confined by their host galaxy's very dense ISM, ot that they are young objects which eventually will evolve into large radio galaxies. A detailed review can be found in O'Dea (1998).

A general requirement for sources classified as CSS is a spectral index of less than -0.5, a source size of less than about 20 kpc, and 1.4 GHz luminosities of more than 10^{25} W m^{-2} Hz^{-1} (O'Dea 1998). S427 has log($L_{1.4}$)=26.1 if z=1 and log($L_{1.4}$)=28.1 if z=7. Its size and luminosity are therefore in good agreement with typical CSS luminosities, if S427 is at high redshifts.

Using VLBI observations of seven strong CSS Tzioumis et al. (2002) detect double-lobed structures in all objects. They also find that in most of their objects more than 50 % of the arcsec-scale flux density is contained in the VLBI images, however, in one case the amount of emission resolved out by the VLBI observations is as high as 70 %.

If S427 indeed is a CSS source or a variant thereof, its infrared properties are expected to be consistent with those of known sources. The infrared properties of CSS sources are not well studied, but Heckman et al. (1994) find that the ratio of IR to radio luminosity of radio galaxies is relatively independent of the object class (FR II, quasar, GPS/CSS, and so on). This was confirmed in similar studies carried out by Hes et al. (1995), and by Fanti et al. (2000). An interesting consequence is that if CSS sources are "frustrated" radio sources with strong interactions with a dense interstellar medium one would expect excess FIR emission from jet-ISM interactions, which has not been found.

Dicken et al. (2008) have recently carried out an investigation of the radio and infrared properties of powerful, radio-loud radio galaxies at intermediate redshifts using literature data, ATCA, VLA and *Spitzer* observations. Their data suggest that the 24 μm flux densities of radio galaxies are one to two orders of magnitude lower than the 1.4 GHz flux densities, independent of object type. Their study includes the four known CSS sources PKS 0252-71, PKS 1151-34, PKS 1814-63 and PKS 1934-63, the radio and infrared properties of which follow the trend of their sample. For S427 that implies that the expected 24 μm flux density would be between 0.2 mJy and 2 mJy. The 1 σ sensitivity of the 24 μm ATLAS/*Spitzer* observations is 252 μJy hence the non-detection of 24 μm emission in the ATLAS survey is consistent with the observations by Dicken et al. (2008).

5. Conclusions

We present the first VLBI image of an Infrared-Faint Radio Source and report the non-detection of three more IFRS discovered in the ATCA 1.4 GHz observations of the ATLAS/ELAIS field. The size, spectrum, and luminosity of the detected IFRS (if it is at high redshift) are consistent with properties of Compact Steep-Spectrum sources. Together with the IFRS detected by Norris et al. (2007) the number of IFRS observed with VLBI is now 5, and the number of detections is 2. These numbers are too small to draw general conclusions on their nature, but they show that observing IFRS with VLBI can help to understand single objects. Furthermore, the detection of compact structures rules out that the two objects detected are just radio lobes of unidentified radio galaxies.

References

Bock, D. C.-J., Large, M. I., & Sadler, E. M. 1999, AJ, 117, 1578
Dicken, D., Tadhunter, C., Morganti, R., et al. 2008, ArXiv e-prints, 803
Fanti, C., Pozzi, F., Fanti, R., et al. 2000, A&A, 358, 499
Heckman, T. M., O'Dea, C. P., Baum, S. A., & Laurikainen, E. 1994, ApJ, 428, 65
Hes, R., Barthel, P. D., & Hoekstra, H. 1995, A&A, 303, 8
Higdon, J. L., Higdon, S. J. U., Weedman, D. W., et al. 2005, ApJ, 626, 58
Lonsdale, C. J., Smith, H. E., Rowan-Robinson, M., et al. 2003, PASP, 115, 897
Middelberg, E., Norris, R. P., Cornwell, T. J., et al. 2008, AJ, 135, 1276
Norris, R. P., Afonso, J., Appleton, P. N., et al. 2006, AJ, 132, 2409
Norris, R. P., Tingay, S. J., Phillips, C., et al. 2007, MNRAS
O'Dea, C. P. 1998, PASP, 110, 493
O'Dea, C. P. & Baum, S. A. 1997, AJ, 113, 148
O'Dowd, M., Urry, C. M., & Scarpa, R. 2002, ApJ, 580, 96
Shepherd, M. C. 1997, in ASP Conf. Ser. 125: Astronomical Data Analysis Software and Systems VI, 77
Tzioumis, A., King, E., Morganti, R., et al. 2002, A&A, 392, 841

Acknowledgements. We thank the staff of the Australian Long Baseline Array for making the observations presented in this paper possible.